

SEPARATION MECHANISM FOR BUBBLES GROWING SLOWLY ON A
HORIZONTAL HEATER FACE

E. I. Nesis and V. I. Komarov

UDC 536.423.1

The relation connecting the shape and volume of a bubble (three-dimensional problem) is studied by a combination of analytical and numerical methods. The mechanism for separation of a bubble from a wetted solid surface is explained and a formula for the separation diameter derived.

The explanation of the mechanism for separation of vapor bubbles from a solid surface is extremely important in the study of boiling and other physicochemical processes [1, 2]. Roughness and wettability of the heater and the rate of bubble growth have a fundamental effect on separation characteristics. The rate of growth, which takes on values of a broad range for various boiling conditions, determines the relative role of dynamic effects in the confinement of bubbles to a solid surface and in their separation. According to estimates made by a number of authors [1], the magnitude of the inertial force of a dynamic reaction of a fluid depends directly on the Jacob number and, consequently, on the ratio $\Delta T/\rho'$. Hence it is clear that one can neglect the hydrodynamic reaction in comparison with static forces which are practically independent of the temperature head ΔT and the vapor density ρ' for small ΔT (initial stages of bubbling boiling) at sufficiently high external pressures.

The kinetics of bubble (drop) growth and separation even in the simpler than general case of slow increase in volume — because of evaporation of liquid (condensation of vapor) — lacks a satisfactory theoretical explanation although this problem has been studied for a long time [3-16].

The application to the solution of this problem of numerical methods alone may not give a physically complete picture of the variation in bubble shape, particularly near separation. An exact analytical solution, which has been successfully carried to completion for the two-dimensional problem [9, 10], entails very great, and possibly insurmountable, difficulties in the three-dimensional case. Because of this, a combination of the analytic method and a numerical solution specially performed on a computer, the data from which was used to justify approximations and check expressions obtained, was employed in this work to study the shape characteristics of three-dimensional bubbles and the mechanism for their separation from a horizontal plane.

During quasistatic growth, the bubble has a shape close to the equilibrium shape at each moment, which ensures a minimum in the sum of the gravitational and surface components of the free energy F for a given bubble volume V . Because of the symmetry of the problem, a bubble on a horizontal plane is a figure of rotation around the vertical axis (Fig. 1a) of some contour $y(x)$ which is determined from the solution of the Euler equation for the corresponding variational problem of a relative extremum [7]:

$$\frac{1}{x} \cdot \frac{d}{dx} \frac{xy'}{(1+y'^2)^{1/2}} = \lambda - \frac{y}{a^2} \quad (1)$$

In Eq. (1), which is one of the forms of the fundamental equation of the theory of capillarity $\alpha = (\sigma/(\rho - \rho'))g)^{1/2}$ is the capillary constant and λ is an undetermined Lagrangian multiplier (with the coefficient σ). Since, as is easily verified, the expression on the left side of Eq. (1) can be represented as the sum of the two principal curvatures of the interface between the liquid and vapor phases, the quantity λ is equated to twice the average curvature of the bubble surface at the base ($y = 0$). In accordance with the treatment of Lagrangian

Translated from *Inzhenerno-Fizicheskii Zhurnal*, Vol. 29, No. 5, pp. 799-807, November, 1975. Original article submitted December 4, 1974.

This material is protected by copyright registered in the name of Plenum Publishing Corporation, 227 West 17th Street, New York, N.Y. 10011. No part of this publication may be reproduced, stored in a retrieval system, or transmitted, in any form or by any means, electronic, mechanical, photocopying, microfilming, recording or otherwise, without written permission of the publisher. A copy of this article is available from the publisher for \$7.50.

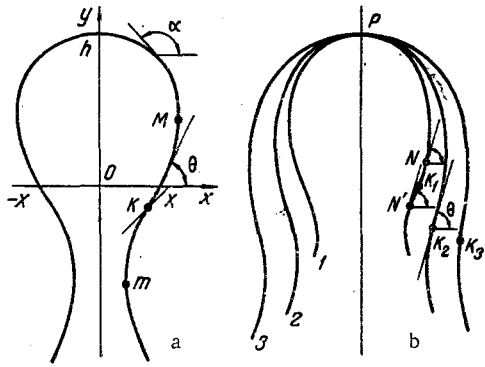


Fig. 1. a) Bubble contour and coordinate system; b) matching of contour apices for numerical integration, $\mu_1 > \mu_2 > \mu_3$.

multipliers in problems of a relative extremum, $\lambda = -(dF/dV)/\sigma$ and as the bubble grows, λ increases starting from infinitely large negative values. The size of a bubble for which $\lambda = 0$ is critical: the total energy reaches a maximum and the bubble "crosses" the potential barrier. As shown by analysis, however, separation of a bubble is not directly related to the vanishing of λ , but to the breakdown of the equilibrium surface shape.

We first consider some obvious results which can easily be obtained for the two-dimensional case. Interest in the dynamics of two-dimensional bubbles has been maintained up until the present time [9, 10, 14, 16]. This can be explained, first, by the fact that, as shown by experiment, one can arrive at qualitatively correct conclusions about the behavior of ordinary three-dimensional bubbles on the basis of the solution of the two-dimensional problem, and, second, by the fact that two-dimensional bubbles (drops) are not pure abstractions and can be realized, for example, in cases where the vapor-liquid system is bounded by two adjacent vertical planes (narrow slit) [16]. An exact solution of the two-dimensional problem with the help of elliptic integrals is given in the form of detailed tables [10], but some results can be obtained without resorting to them.

For the transition to the two-dimensional problem, one should eliminate one of the principal curvatures in the term $y'/(1+y'^2)^{1/2}x$ on the left side of Eq. (1):

$$\frac{d}{dx} \cdot \frac{y'}{(1+y'^2)^{1/2}} = \lambda - \frac{y}{a^2}. \quad (2)$$

The first integral of Eq. (2) has the form [6]

$$2\sin^2 \frac{\alpha}{2} = \frac{h^2 - y^2}{2a^2} + \lambda(y - h), \quad (3)$$

where α is the angle between the tangent at any point on the bubble contour (Fig. 1a) and the horizontal axis. Then the parameter λ is simply expressed through the bubble height h and the contact angle θ [7]:

$$\lambda = \frac{h}{2a^2} - \frac{2}{h} \cos^2 \frac{\theta}{2}. \quad (4)$$

It is obvious that in both the two-dimensional and three-dimensional cases separation of a bubble along a section of finite area is impossible because the surface energy would then increase discontinuously by a finite amount, while the volume gravitational energy would decrease by an infinitely small amount with separation of the upper portion. Separation can occur only at nodes of the liquid-vapor interface in two cases: a) a node is formed at the boundary with a solid wall as the result of complete contraction of the bubble base; b) a node is produced by contraction to a point of a neck in the contour present above the plane. In the first type of separation, the bubble separates as a whole; in the second type, a portion of the vapor volume remains on the plane.

To find the conditions for the existence of a neck above the solid surface, one should determine the ordinates y_e of the extremum points M and m on the contour, which correspond to $\alpha = \pi/2$, from the quadratic equation which is obtained by using Eq. (3):

$$y_e^2 - 2a^2\lambda y_e + 2a^2 + 2a^2\lambda h - h^2 = 0.$$

Considering the relation between λ and h from Eq. (4), we arrive at

$$y_e = a^2\lambda \left(1 \pm \sqrt{1 + \frac{2\cos \theta}{\lambda^2 a^2}} \right). \quad (5)$$

Equation (5) indicates that for good wettability ($\cos \theta > 0$) a maximum x (the point M) always is present above the plane, but a minimum (point m) cannot appear whatever the value of h ,

since the two roots have different signs in this case for any λ . Consequently, the bubble cannot separate along a neck but separates completely. For small bubbles ($\lambda < 0$) on an unwettable surface the ordinates of both the maximum and minimum are negative. With further growth of the bubble, which is accompanied by an increase in λ , the shape of the contour $x(y)$ is such that there is generally neither a maximum nor minimum on it (for $\lambda^2 a^2 < -2 \cos \theta$). Only for sufficiently large positive values $\lambda a > \sqrt{2} |\cos \theta|$ does the contour have both greatest expansion and a neck above the plane.

Representing Eq. (2) in the following form:

$$d(\sin \alpha) = \lambda dx - \frac{y dx}{a^2} \quad (2')$$

and taking the definite integral between the limits $x = 0$ and $x = X$, we obtain

$$\frac{S}{a^2} = \lambda X + \sin \theta, \quad (6)$$

where S is the bubble area bounded by the contour.

In the region of small contact angles (up to 50°), it has been shown [9, 10] that during the growth of a bubble its base first expands and then completely contracts. In the next region of contact angles (up to 90°), the time for breakdown of equilibrium is associated with the appearance of an inflection point in the contour at the base and with the vanishing of λ . For both these cases, it is easy to obtain from Eq. (6)

$$D_0 = \sqrt{\frac{4S_0}{\pi}} = \frac{2}{\sqrt{\pi}} (\sin \theta)^{1/2} a \quad (7)$$

for the equivalent separation diameter.

We now turn to an analysis of the considerably more complex problem of the evolution of a three-dimensional bubble. Transforming the original equation (1) to

$$d \left(\frac{x}{(1+x'^2)^{1/2}} - \frac{x^2 y}{2a^2} - \frac{\lambda x^2}{2} \right) = - \frac{1}{2a^2} x^2 dy \quad (8)$$

and taking the definite integral between the limits $y = 0$ and $y = h$, we obtain a relation connecting one of the most important bubble dimensions — the radius X of the base — to the volume V and the values of the physical parameters

$$\lambda X^2 + 2 \sin \theta X = \frac{V}{\pi a^2}. \quad (9)$$

We solve this equation with respect to X and transform to dimensionless quantities ($\bar{X} = X/a$, $\bar{V} = V/a^3$, $\bar{\lambda} = \lambda a$):

$$\bar{X} = - \frac{\sin \theta}{\bar{\lambda}} \left(1 \pm \sqrt{1 + \frac{\bar{\lambda} \bar{V}}{\pi \sin^2 \theta}} \right). \quad (10)$$

Analysis of the limiting cases of a small bubble (or the case of weightlessness) and of a large bubble ($\bar{\lambda} \rightarrow 0$) makes it possible to determine the correct choice of sign in Eq. (10). The plus sign is taken from the beginning of bubble growth until there is an inflection point in the contour. Both roots of Eq. (9) coincide at the time when an inflection point in the contour appears at the base of the bubble; the quantity λ becomes equal to one of the principal curvatures, $-\sin \theta/X$. For a bubble continuing to grow after this, the minus sign in Eq. (10) must be taken.

Equation (10) expresses the complex dependence of \bar{X} on the volume \bar{V} (or the bubble height \bar{h}) and on the contact angle, since the factor $\bar{\lambda}$ appearing in Eq. (10) is a function of these same quantities in a form which has yet to be established. However, use of the variational treatment of λ , in accordance with which $\lambda = -(dF_\sigma/dV)/\sigma$ for bubbles that are not too large, and of the analogy with the exact form of λ for the two-dimensional problem makes it possible to express the Lagrangian multiplier in the first approximation as

$$\bar{\lambda} = - \frac{4 \cos^2 \frac{\theta}{2}}{\bar{h}}. \quad (11)$$

Considering the general nature of the variation of $\bar{\lambda}$ defined by Eq. (11), we employ along with it the relationships $\bar{\lambda}(\bar{h})$ and $\bar{V}(\bar{h})$ determined by a numerical method for analysis of the behavior of the base of a growing bubble.

In the numerical integration on a Minsk-32 computer of the system of two differential equations of first order obtained from Eq. (1), we determined the coordinates and curvature of the integral curve, the angle α for the slope of the tangent, and the volume of the bubble — a body of rotation about the vertical axis of the portion of the integral curve from the apex to a point at which α is equal to a given contact angle. Since the portions of contours of bubbles with different θ adjacent to the apex of the integral curve coincide, it is convenient to select a common origin for numerical integration (Fig. 1b) and to take twice the average curvature μ at the apex as an arbitrarily established parameter. On each integral curve, the minimum value of the tangent slope $\alpha_{\min} = \alpha_{\min}(\mu)$ corresponds to the inflection point (on curves with large μ , the first inflection point from the apex). As μ decreases, α_{\min} increases monotonically. For given θ , therefore, the contours of bubbles of different size are formed by portions only of those curves for which $\mu \geq \mu^*$ [$\alpha_{\min}(\mu^*) = \theta$]. When $\mu > \mu^*$, there are always two points on the integral curve where $\alpha = \theta$ which are, respectively, located above and below the inflection point of a given curve. In Fig. 1b these are the points N and N' on curve 1 for which $\alpha(N) = \alpha(N') = \alpha_{\min}(\mu_2) = \theta$; $\alpha_{\min}(\mu_3) \equiv \alpha(K_3) > \theta$.

As the bubble grows, μ decreases at first and the upper of the points with $\alpha = \theta$ are the end points of the contours lying in the boundary with the base of the bubble. When μ reaches the value μ^* , an inflection point is located on the contour at the base. Further shifting of the end of the contour continues along points such as N' with an increase in the curvature at the apex; the bubble is considerably different in shape from a spherical segment, an inflection point is present in the contour above the base, and also a neck when μ is large enough. One can determine whether a contour with the point N' on the perimeter of wetting corresponds to a stable form of bubble by considering the change in the volume V. If during the evolution of shape described, an initially increasing volume, having reached a maximum value V_{\max} , decreases, it is clear that the resultant shape is unstable. In this case, the portion PN' of the integral curve does not realize a minimum but rather a relative maximum of the total energy for the class of curves satisfying the original differential equation.

According to data obtained from a numerical solution for angles θ less than some θ_0 near 70° , an increase in volume occurs up to the appearance of an inflection point in the contour at the boundary with the base. For larger θ , the bubble continues to grow after this time and V_{\max} is reached with an inflection point present above the base.

To explain the reasons for this difference, we consider Eq. (10) for \bar{X} (before the appearance of an inflection point in a contour with the plus sign). Considering the kind of variation in $\bar{\lambda}$ as \bar{h} increases, one can conclude that the first factor on the right side ($-\sin \theta / \bar{\lambda}$) increases along with bubble height, while the sum in parentheses decreases: the product $\bar{\lambda}\bar{V}$, being negative, increases with respect to modulus, since \bar{V} grows more rapidly (at first, $\sim \bar{h}^3$) than $|\bar{\lambda}|$ decreases. The behavior of the function $\varphi \equiv |\bar{\lambda}\bar{V}|$ for $\theta = 30^\circ$ and $\theta = 100^\circ$ is plotted in Fig. 2a,b on the basis of data from the numerical solution. Initially, the first effect predominates and \bar{X} increases, but the decrease in the factor inside the parentheses becomes more important and the width of the base is reduced after passing through a maximum. Such behavior of the bubble base is in agreement with experimental observations [2, 18] and with the results of computer calculations on which the curves for the dependence of \bar{X} on \bar{h} shown in Fig. 2 are based.

The vertical line A in Fig. 2 denotes the time of appearance of an inflection point in the contour at the base of a bubble with a bubble height \bar{h}^* ; the line B denotes the achievement of \bar{V}_{\max} by the bubble, which is a criterion for breakdown of equilibrium and subsequent separation of the bubble [up to this limit, the curves $\varphi(\bar{h})$ and $\bar{X}(\bar{h})$ are shown as solid lines] the line C denotes the maximum value of \bar{h} for a given θ for all stable and unstable forms of the integral curves — $(d\bar{X}/d\bar{h}) = -\infty$. The dashed portions of the $\varphi(\bar{h})$ and $\bar{X}(\bar{h})$ curves correspond to unstable forms of contours.

At \bar{h}^* , φ reaches its greatest value, $\pi \sin^2 \theta$. The manner in which φ approaches this value is important for the separation mechanism. If $(d\varphi/d\bar{h})_* \neq 0$, i.e., the curve approaches the line $\varphi = \pi \sin^2 \theta$ at an angle, the rapidity of the change in radius of the base with increase in height tends to $-\infty$ as shown by an analysis of the expression for the derivative $d\bar{X}/d\bar{h}$. If indeed $(d\varphi/d\bar{h})_* = 0$, i.e., the curve $\varphi(\bar{h})$ is tangent to the line $\varphi = \pi \sin^2 \theta$, the derivative $d\bar{X}/d\bar{h}$ has no singularities.

The first case is observed for small θ and the limits A, B, and C then merge as is clear from Fig. 2a. Furthermore, the point of division of the $\varphi(\bar{h})$ curve into solid and dashed

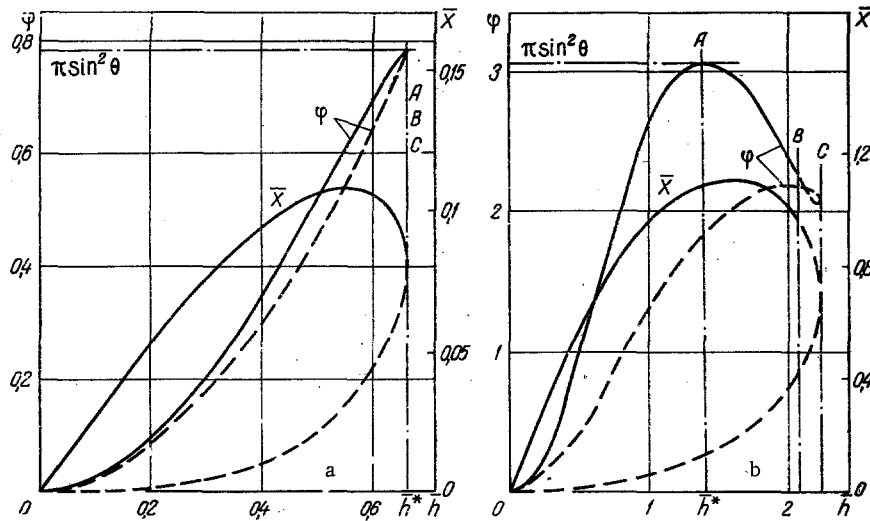


Fig. 2. Dependence of φ and radius \bar{X} of bubble base on height \bar{h} based on data from computer solution for contact angles $\theta = 30^\circ$ (a) and $\theta = 100^\circ$ (b).

TABLE 1. Separation (maximum equilibrium) Diameter of Bubbles

θ , deg	D_0/a		
	from numerical solution	from Fritz formula	from Eq. (14)
18.95	0,404	0,394	0,424
30.0	0,633	0,624	0,634
42.6	0,896	0,886	0,890
54.15	1,13	1,13	1,12
70.9	1,47	1,48	1,42
85.0	1,76	1,77	1,66

branches (at \bar{h}^*) is a singularity. Physically, it is clear that the trend to ∞ for the rate of decreases must have as a consequence complete constriction [which occurs in nonequilibrium fashion and is therefore not described by Eq. (10)]. Such a mechanism of bubble separation is apparently only possible for those values of the contact angle $\theta < \theta_0$ for which the rate of contraction of the base, although not going to ∞ , becomes sufficiently great.

The second case occurs for large θ . The appearance of an inflection point in the contour occurs long before the achievement of \bar{V}_{\max} and is not associated with any peculiarities in the behavior of \bar{X} ; the base of the bubble is still expanding at this time for $\theta > 90^\circ$. When \bar{h} becomes greater than \bar{h}^* , φ begins to decrease so that Eq. (10) does not lose meaning. With further increase in V , the inflection point rises above the plane and the slope of the tangent at this point increases. Such changes of the inflection point in a contour lead to transformation into a neck in the contour [7]; with contraction of this neck, the second type of separation occurs (it is obvious that this occurs in a nonequilibrium stage just like the total contraction of the base when $\theta < \theta_0$).

The fact that the cause of bubble separation is breakdown of equilibrium shape is reflected in the circumstance that, based on data from the numerical solution, the quantity $\bar{\lambda}$ when $\bar{V} = \bar{V}_{\max}$ still has negative values (for $\theta < 120^\circ$) and for small θ is far from reaching the value $\bar{\lambda} = 0$, which corresponds to the limit for three-dimensional stability of a bubble.

In the case of total separation, one can estimate the size of bubbles at the time of breakdown of equilibrium, relating it to the appearance of an inflection point on the contour. We use Eq. (11), which from the computer data is satisfied to an accuracy of a few percent for $\theta < 70^\circ$ up to $\bar{h} = \bar{h}^*$. Then the condition for breakdown of equilibrium takes the form

$$\bar{V}_{\max} = \pi \sin^2 \frac{\theta}{2} \bar{h}^*. \quad (12)$$

If one assumes that the shape of the bubble for small θ differs slightly from a spherical segment (except for the region near the base), the volume of which is $V = \frac{1}{6}\pi h^3 [1 + 3 \tan^2(\theta/2)]$, we obtain for the diameter of a sphere of volume V_{\max} (the separation diameter)

$$D_0 = \sqrt[6]{6} \sin \frac{\theta}{2} \left(1 + 3 \operatorname{tg}^2 \frac{\theta}{2}\right)^{-1/6} a. \quad (13)$$

Discarding the small corrections, we obtain a simple expression for the separation diameter,

$$D_0 \approx \sqrt[6]{6} \cdot \sin \frac{\theta}{2} a. \quad (14)$$

As the data in Table 1 show, calculations based on the approximate analytic expression (14) in its region of applicability yield practically the same results as those from the semi-empirical Fritz formula $D_0 \approx 0.0208\theta^{3/2}\alpha$ [17] obtained on the basis of a numerical solution [3] and extrapolated to the region of small θ .

Note that the limit of bubble equilibrium for good wettability used by us in the determination of D_0 is reached earlier, though not much earlier, than the limit of stability with respect to perturbations of the interface calculated in [12].

As follows from Eq. (10), the radius of the base of a bubble at the time of breakdown of equilibrium is

$$\bar{X}^* = \frac{\bar{V}_{\max}}{\pi \sin \theta}. \quad (15)$$

If the growth of the bubble occurs on a surface that is not smooth but contains microcavities (voids), they can have an effect on separation size only if the radius r of the mouth of a void (which is assumed to be conical) is greater than X^* . Indeed, since breakdown of equilibrium occurs during contraction of the base, $X_{\max} > X^*$ and in the expansion stage, a base having reached the lip of a cavity slides along a smooth surface. Subsequent changes in bubble shape are completely unrelated to the presence of microcavities as long as the line of wetting does not once again reach the lip before the time of breakdown of equilibrium. Using the above, we obtain for the critical radius r^* of the mouth of a void, which divides separation from a smooth surface (when $r < r^*$) and separation from the lip of a void with good wettability, the expression

$$r^* = \frac{\sqrt[6]{6}}{2} \sin \frac{\theta}{2} \operatorname{tg} \frac{\theta}{2} a. \quad (16)$$

This expression is in good agreement with data for r^* [13] obtained by a numerical method.

NOTATION

σ , surface tension; ρ, ρ' , densities of liquid and vapor; g , acceleration of gravity; a , capillary constant; θ , contact angle; ΔT , temperature head; Ja , Jacob number; x and y , coordinates; $y' = dy/dx$; $x' = dx/dy$; $x'' = d^2x/dy^2$; α , angle of tangent with the horizontal at an arbitrary point on the contour; X and h , base radius and height of bubble; S , area bounded by contour of two-dimensional bubble; λ , Lagrangian multiplier; V , bubble volume; $\bar{X} = X/a$; $\bar{h} = h/a$; $\bar{V} = V/a^3$; $\bar{\lambda} = \lambda a$; $\varphi = |\bar{\lambda}\bar{V}|$; μ , curvature of bubble surface at apex; F, F_0 , total and surface free energy of bubble; D_0 , separation diameter; r , radius of microcavity mouth.

LITERATURE CITED

1. E. I. Nesis, *Boiling Liquids* [in Russian], Nauka, Moscow (1973).
2. B. N. Kabanov and A. N. Frumkin, *Zh. Fiz. Khim.*, 4 (1933).
3. F. Bashforth and J. C. Adams, *An Attempt to Test the Theories of Capillary Action*, Cambridge University Press (1883).
4. I. Wark, *J. Phys. Chem.*, 37, 623 (1933).
5. W. Fritz, *Phys. Z.*, 36, 379 (1935).
6. E. I. Nesis, *Zh. Tekh. Fiz.*, 22, 1506 (1952).
7. E. I. Nesis, *Dokl. Akad. Nauk SSSR*, 165, 871 (1965).
8. E. I. Nesis, V. N. Tokmakov, and T. S. Chigareva, *Izv. Akad. Nauk SSSR, Énergetika i Transport*, No. 2, 146 (1967).
9. E. I. Nesis and T. S. Chigareva, *Izv. Vyssh. Uchebn. Zaved., Fiz.*, No. 7, 135 (1969); *Zh. Fiz. Khim.*, 46, 1442 (1972).
10. T. S. Chigareva, *Author's Abstract of Candidate's Dissertation*, Kabardine-Balkarian State University, Nal'chik (1970).

11. M. A. Belyaeva, L. A. Slobozhanin, and A. D. Tyuptsov, in: Introduction to Dynamics of Bodies Containing Liquid under Weightless Conditions [in Russian], Izd. Vychisl. Tsentr Akad. Nauk SSSR (1968).
12. L. A. Slobozhanin and A. D. Tyuptsov, Izv. Akad. Nauk SSSR, Mekh. Zhidk. Gaza, No. 4, 3 (1973); No. 4, 74 (1974).
13. Yu. A. Kirichenko, L. A. Slobozhanin, and N. S. Shcherbakova, Determination of Vapor Bubble Sizes [in Russian], Preprint FTNT, Akad. Nauk Ukrainian SSR, Khar'kov (1974).
14. K. Tamada and Y. Shibaoka, J. Phys. Soc. Jap., 16, 1249 (1961).
15. K. Hida and T. Nakanishi, J. Phys. Soc. Jap., 28, 1336 (1970).
16. E. Pitts, J. Fluid Mech., 59, 753 (1973).
17. V. P. Isachenko, B. A. Oispova, and A. S. Sukomel, Heat Transfer [in Russian], Énergiya, Moscow (1969), p. 286.
18. E. I. Aref'eva and I. T. Alad'ev, Inzh.-Fiz. Zh., 1, 11 (1958).

INVESTIGATION OF THE HEAT AND MASS TRANSFER DURING
SUBLIMATION OF ICE BY THE METHOD OF "THERMAL SHOCK"

D. P. Lebedev and Lieh-Kue Ki

UDC 536.422.1

Experimental results are presented and computational dependences are obtained for the heat and mass transfer during sublimation of ice.

The experimental and theoretical investigations of the ice sublimation mechanism in a vacuum known at this time [1-5] for thermoradiation energy fluxes supplied to the sublimation zone examine the "stationary" sublimation process (first period) characterized by a constant sublimation rate and a constant temperature distribution in the specimen with time.

In reality, the process of sublimation parameter buildup (the heating period) [6] precedes the first period. This period is ordinarily eliminated completely [3-5, 13] in the traditional method of investigating the sublimation process. The complexity of these investigations is associated with the fact that the radiator itself is heated during the heating period and the radiation heat exchange of the subliming material with the radiator, with the walls of the vacuum chamber and other measuring attachments varies. In order to eliminate all secondary phenomena and to obtain more accurate experimental results, as well as to approximate the experimental results to the classical physical problem, we used a more perfect model with instantaneous insertion of an energy supply for the complex investigation of sublimation processes with thermoradiation supply of heat [6, 7]. This method of organizing the energy supply affords a possibility of obtaining well-founded experimental data,* which significantly expand the possibilities of a mathematical-physics analysis.

Experimental Model

The experimental model (Fig. 1) for the investigation of nonstationary sublimation processes in a vacuum was a structural modification of the model examined in [6], which consists of using two symmetric infrared radiators to organize the thermoradiation energy supply. The investigations were conducted at pressures from 1 to 10^{-3} mm Hg.

The experimental ice specimen 1 is cylindrical in shape (32 mm in diameter, 16 mm in thickness). To exclude uncheckable radiant fluxes from the specimen (vacuum chamber walls,

*We investigate in this paper the ice sublimation process under the effect of an "infinite" duration heat pulse which we call the "thermal shock" method.

Moscow Power Institute. All-Union Scientific-Research Biotechnical Institute, Moscow. Translated from Inzhenerno-Fizicheskii Zhurnal, Vol. 29, No. 5, pp. 808-813, November, 1975. Original article submitted December 10, 1973.

This material is protected by copyright registered in the name of Plenum Publishing Corporation, 227 West 17th Street, New York, N. Y. 10011. No part of this publication may be reproduced, stored in a retrieval system, or transmitted, in any form or by any means, electronic, mechanical, photocopying, microfilming, recording or otherwise, without written permission of the publisher. A copy of this article is available from the publisher for \$7.50.